Catalysis Science & Technology

Well-Defined, Air- and Moisture-Stable Palladium–Imidazo[1,5- a]pyridin-3-ylidene Complexes: A Versatile Catalyst Platform for Cross-Coupling Reactions by L-Shaped NHC Ligands

Journal:	*Catalysis Science & Technology*
Manuscript ID	CY-ART-06-2022-001136.R1
Article Type:	Paper
Date Submitted by the Author:	17-Aug-2022
Complete List of Authors:	Zhou, Tongliang; Rutgers University, Chemistry Gao, Pengcheng; Rutgers University, Chemistry Bisz, Elwira; Opole University, Department of Chemistry Dziuk, Blazej; University of Science and Technology, Chemistry Lalancette, Roger; Olson Laboratories, Rutgers University, Department of Chemistry Szostak, Roman; University of Wroclaw, Chemistry Szostak, Michal; Rutgers University, Department of Chemistry

Catalysis Science & Technology

ARTICLE

Well-Defined, Air- and Moisture-Stable Palladium–Imidazo[1,5-*a*]pyridin-3-ylidene Complexes: A Versatile Catalyst Platform for Cross-Coupling Reactions by L-Shaped NHC Ligands

Received 00th January 20xx,
Accepted 00th January 20xx

DOI: 10.1039/x0xx00000x

www.rsc.org/

Tongliang Zhou,[a] Pengcheng Gao,[a] Elwira Bisz,[b] Błażej Dziuk,[c] Roger Lalancette,[a] Roman Szostak,[d] and Michal Szostak*,[a]

We describe the development of [(NHC)Pd(cinnamyl)Cl] complexes of ImPy (ImPy = imidazo[1,5-*a*]pyridin-3-ylidene) as a versatile class of precatalysts for cross-coupling reactions. These precatalysts feature fast activation to monoligated Pd(0) with 1:1 Pd to ligand ratio in a rigid imidazo[1,5-*a*]pyridin-3-ylidene template. Steric matching of the C5-substituent and N2-wingtip in the catalytic pocket of the catalyst framework led to the discovery of ImPyMesDipp as a highly reactive imidazo[1,5-*a*]pyridin-3-ylidene ligand for Pd-catalyzed cross-coupling of nitroarenes by challenging C–NO_2 activation. Kinetic studies demonstrate fast activation and high reactivity of this class of well-defined ImPy–Pd catalysts. Structural studies provide full characteristics of this new class of imidazo[1,5-*a*]pyridin-3-ylidene ligands. Computational studies establish electronic properties of sterically-restricted imidazo[1,5-*a*]pyridin-3-ylidene ligands. Finally, a scalable synthesis of C5-substituted imidazo[1,5-*a*]pyridin-3-ylidene ligands through Ni-catalyzed Kumada cross-coupling is disclosed. The method obviates chromatographic purification at any of the steps, resulting in a facile and modular access to ImPy ligands. We anticipate that well-defined [Pd–ImPy] complexes will find broad utility in organic synthesis and catalysis for activation of unreactive bonds.

Introduction

N-Heterocyclic carbenes (NHCs) have found expansive applications in organic synthesis and catalysis since the first isolation of an archetypal free carbene by Arduengo in 1991.[1-7] The strong σ-donating abilities and easily tunable steric differentiation make them quintessential ligands for transition-metal-catalysis and main group chemistry.[7-12] The invention of new NHC ligands by (1) N-wingtip modification, (2) backbone alteration, or (3) ring remodeling, has continuously been a key way to profoundly change the electronic and steric properties of NHCs. Successful examples in this field include the discovery of cyclic(alkyl)(amino)carbenes (CAACs),[13] sterically-demanding bioxazoline carbenes (IBiox),[14] abnormal NHCs (aNHCs),[15-16] mesoionic carbenes (MICs),[17-18] among many others.[19-20]

Imidazo[1,5-*a*]pyridin-3-ylidenes (ImPy), first reported in 2005, feature unique architecture leading to a sterically demanding environment around the metal center when the C5 position is substituted by an aryl group (**Figure 1A**).[21-22] In light of appealing attributes of sterically-restricted NHC ligands,[23-25] we anticipated that highly attractive ligands could be obtained by steric matching of the restricted C5 and flexible N2-substitutes, providing a powerful strategy for the invention of new chemical technologies for bond activation.

A major advancement in palladium-based catalyst design is the development of well-defined Pd(II)–precatalysts, where Pd to ligand ratio is 1:1 (**Figure 1B**).[26] This Pd-catalyst design strategy offers a major advantage over *in situ* formed catalysts due to the stability of Pd–complexes and high price of ancillary ligands (*cf*. Pd source).[27-36] In this context, Pd(NHC)(cin)Cl,[32] Pd–PEPPSI,[33] SingaCycle A1–A3,[34] (CAAC)Pd(allyl)Cl,[35] and Buchwald palladacycles G1–G4[36] have emerged as established benchmarks for palladium-catalyzed cross-coupling reactions, and many of them are now commercially available.

On the other hand, nitroarenes (Ar–NO_2) are highly attractive electrophiles for cross-coupling reactions due to their availability by S_EAr nitration technology complementary to aryl halides, low price as chemical feedstocks and orthogonal reactivty.[37] The direct utilization of nitroarenes as coupling partners in cross-coupling reactions by Ar–NO_2 oxidative addition is scarce, and the ligands used for the activation of C–N bond in nitroarenes were initially limited to BrettPhos analogues.[38-50]

[a]*Department of Chemistry, Rutgers University, 73 Warren Street, Newark, NJ 07102, USA. E-mail: michal.szostak@rutgers.edu.*
[b]*Department of Chemistry, Opole University, 48 Oleska Street, Opole 45-052, Poland*
[c]*Department of Chemistry, University of Science and Technology, Norwida 4/6, Wroclaw 50-373, Poland*
[d]*Department of Chemistry, Wroclaw University, F. Joliot-Curie 14, Wroclaw 50-383, Poland*

†Electronic Supplementary Information (ESI) available: Experimental details and characterization data. See DOI: 10.1039/x0xx00000x

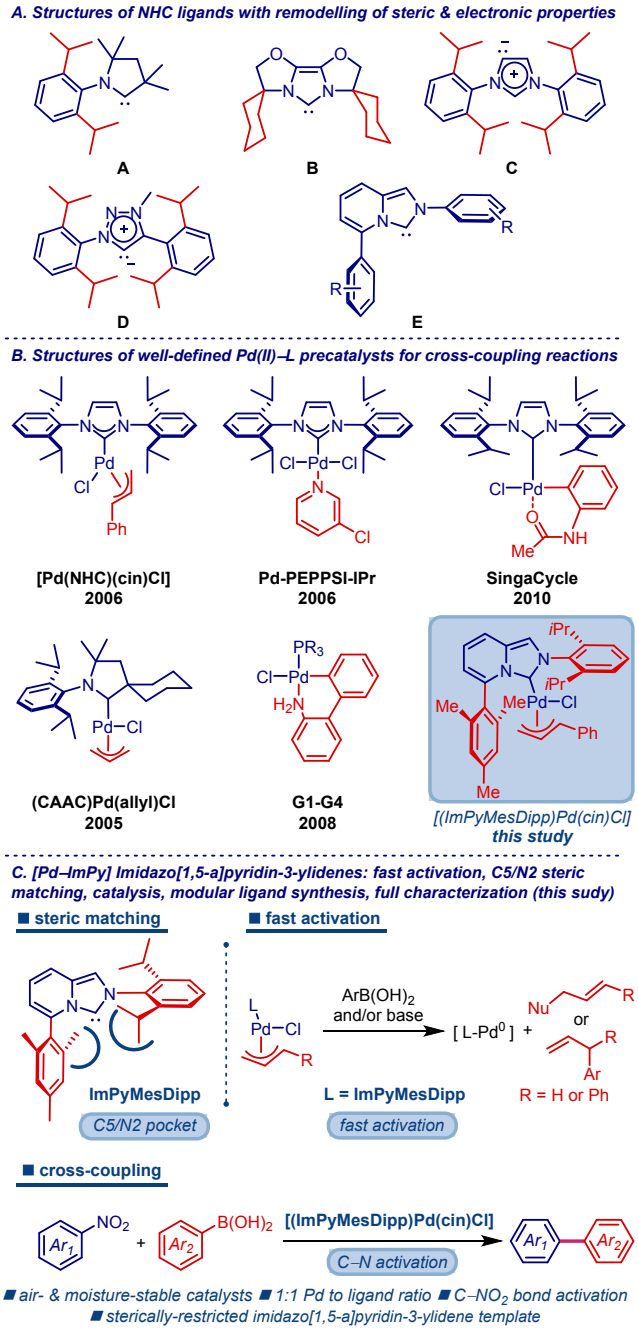

Figure 1. (A) Electronic and structural remodelling of NHC ligands. (B) State-of-the art Pd(II) precatalysts in cross-coupling reactions. (C) Pd(II)–ImPy and steric-matching of [(ImPyMesDipp)Pd(cin)Cl] as air-stable, fast-activating, sterically-restricted Pd(II)–NHC precatalysts.

Subsequently, C5-substituted ImPy were found as active ligands for cross-coupling of nitroarenes.[51-53] However, the protocols relied on large excess of ligands to Pd. Further, long reaction time was required due to slow activation of the putative "Pd(NHC)(acac)Cl" species generated *in situ*.

We reasoned that the key limitations would be addressed by (1) the development of well-defined, fast-activating [(NHC)Pd(cinnamyl)Cl] complexes of ImPy ligands, which would be bench-stable, yet easily activated to NHC–Pd(0) in the presence of arylboronic acid and base, and (2) steric matching of the C5 restricted and N2 flexible substituents to define catalytic pocket for elementary cross-coupling steps (**Figure 1C**). We report the development of [(NHC)Pd(cinnamyl)Cl] complexes of ImPy (ImPy = imidazo[1,5-*a*]pyridin-3-ylidene) as a versatile class of precatalysts for cross-coupling reactions. Most crucially, these air- and bench-stable, well-defined precatalysts feature fast activation to monoligated Pd(0) with 1:1 Pd to ligand ratio in a rigid imidazo[1,5-*a*]pyridin-3-ylidene framework. Catalyst synthesis, kinetic and catalytic studies, full characterization as well as practical and scalable synthesis by Ni-catalyzed Kumada cross-coupling of this class of imidazo[1,5-*a*]pyridin-3-ylidene ligands is disclosed.[54] This study opens the door to activation of unreactive bonds in organic synthesis by well-defined ImPy–Pd catalysts.

Results and discussion

Design Plan. Based on our previous studies on Pd–NHC catalysis,[23-25,28-31] we realized that there should be a precise steric match between the *rigid C5* and *flexible N2* substituents of the catalytic pocket of transition-metal-complexes of imidazo[1,5-*a*]pyridin-3-ylidenes.

A library of C5-Aryl/N2-Aryl imidazo[1,5-a]pyridinium salts with a systematic variation of the C5 and N2 substitution critical to catalysis, namely ImPyMesMes·HCl (**1a**), ImPyMesDipp·HCl (**1b**), ImPyTrippMes·HCl (**1c**), and ImPyTrippDipp·HCl (**1d**) were selected for the initial study (**Figure 2**). The Suzuki-Miyaura cross-coupling of nitroarenes was selected because it is a novel method to activate C–NO_2 bonds, and nitroarenes represent a highly attractive class of orthogonal electrophiles to aryl halides prepared by S_EAr nitration of benzene derivatives. At present, very few methods for the biaryl coupling of nitrobenzenes have been reported.[40, 52-53, 55] It should be noted that (**1c**) is a privileged ligand for the biaryl coupling of nitroarenes reported previously. NHC ligands without steric hindrance at the ortho-position of the C5-substituent are unreactive (not shown).

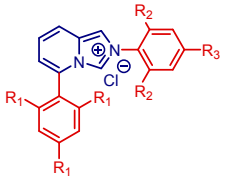

1a, ImPyMesMes•HCl, $R_1 = R_2 = R_3 = Me$
1b, ImPyMesDipp•HCl, $R_1 = Me$, $R_2 = iPr$, $R_3 = H$
1c, ImPyTrippMes•HCl, $R_1 = iPr$, $R_2 = R_3 = Me$
1d, ImPyTrippDipp•HCl, $R_1 = R_2 = iPr$, $R_3 = H$

Figure 2. Structures of imidazo[1,5-a]pyridin-3-ylidene ligands used in this study.

The in situ protocol was first used to screen the selected imidazo[1,5-*a*]pyridin-3-ylidene ligands (Table 1).

4-Nitroanisole and phenylboronic acid were selected as model substrates. Our initial optimization showed that the classical imidazolium salts (IMes·HCl, IPr·HCl) and

imidazolinium salts (SIMes·HCl, SIPr·HCl) were totally ineffective for this transformation, resulting in the recovery of

Table 1. Initial Optimization[a]

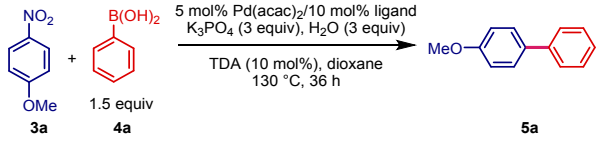

entry	ligand	yield (%)[b]
1	IMesHCl	0
2	SIMesHCl	0
3	IPrHCl	0
4	SIPrHCl	0
5	ImPyMesMes·HCl	13
6	ImPyMesDipp·HCl	33
7	ImPyTrippMes·HCl	47
8	ImPyTrippDipp·HCl	18

[a]Conditions: 4-nitroanisole (1.0 equiv), benzeneboronic acid (1.5 equiv), $Pd(acac)_2$ (5 mol%), ligand (10 mol%), K_3PO_4 (3.0 equiv), H_2O (3.0 equiv), TDA (10 mol%), dioxane (0.2 M), 130 °C, 36 h. [b]GC/NMR yield. TDA = tris(3,6-dioxaheptyl)amine.

nitroarene (Table 1, entries 1-4). Moreover, the screening of imidazo[1,5-*a*]pyridinium salts revealed that both the least sterically-hindered ImPyMesMes·HCl (13% yield) and the most sterically-demanding ImPyTrippDipp·HCl (18% yield) are less effective than ImPyMesDipp·HCl (33% yield) and ImPyTrippMes·HCl (47% yield) (Table 1, entries 5-8). The yield for ImPyTripp-Mes·HCl was not improved by changing the conditions or prolonging the reaction time (not shown).

Synthesis of Pd(II)–NHC Complexes. Next, we sought to prepare well-defined Pd(II)–NHC complexes using cinnamyl ancillary ligands. Cinnamyl ancillary ligands were selected due

Scheme 1. Synthesis of Pd(II)–NHC Complexes[a]

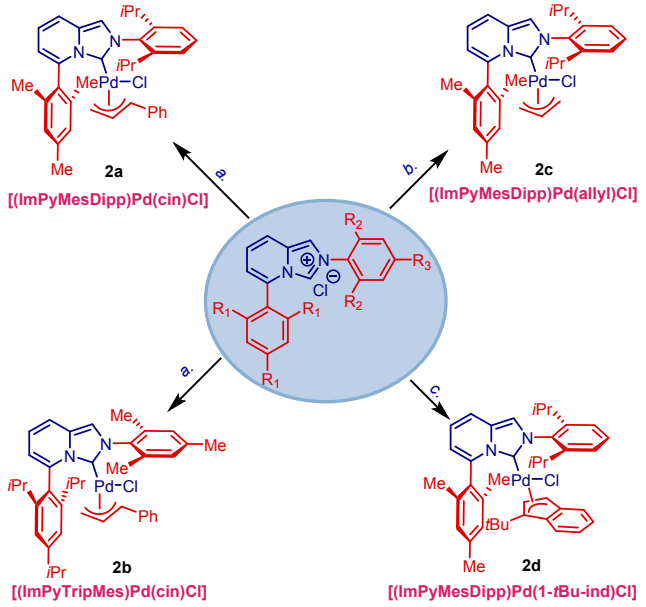

[a]Conditions: (a) $[Pd(cin)Cl]_2$ (0.5 equiv), KO*t*Bu (1.4 equiv), THF (0.1 M), 23 °C, 3 h, 73% (**2a**), 71% (**2b**). (b) $[Pd(allyl)Cl]_2$ (0.5 equiv), KO*t*Bu (1.4 equiv), THF (0.1 M), 23 °C, 3 h, 78%. (c) $[Pd(1\text{-}t\text{Bu-ind})Cl]_2$ (0.5 equiv), KO*t*Bu (1.4 equiv), THF (0.1 M), 23 °C, 3 h, 37%.

to their well-established capacity to serve as supporting ligands to Pd(II)–NHC and Pd(II)–phosphine complexes and because many different R–allyl ligands are available for tuning the reactivity of Pd(II) complexes.[32]

Thus, although the reaction of imidazo[1,5-a]pyridinium salt ImPyMesDipp·HCl with the palladium cinnamyl dimer $[\{Pd(cin)(\mu\text{-}Cl)\}_2]$ in the presence of K_2CO_3 in acetone at reflux failed to give the desired product,[56] we were delighted to find that the desired ImPy–ligated Pd(II) complex [(ImPyMesDipp)Pd(cin)Cl] (**2a**) was successfully obtained in 73% yield after 3 hours at room temperature when we switched to a stronger potassium *tert*-butoxide base and THF as a solvent (**Scheme 1**).

Following similar procedure, complex [(ImPyTripp-Mes)Pd(cin)Cl] (**2b**) from the privileged ImPyTrippMes ligand was prepared (**Scheme 1**). We have also synthesized well-defined complexes [(ImPyMesDipp)Pd(allyl)Cl] (**2c**) and [(ImPyMesDipp)Pd(1-*t*Buind)Cl] (**2d**) bearing allyl and 1-*t*-Bu-indenyl ancillary ligands utilizing the corresponding Pd dimer precursors. The yield for complex (**2d**) was comparatively lower, which we attribute to the excessive steric hindrance of the ancillary ligand.[57] Importantly, all complexes were found to be air- and moisture-stable, with no notable decomposition detected after storing on the bench-top for over 6 months.

Interestingly, in ^1H and ^{13}C NMR we observed two isomers namely endo-, and exo- forms in **2a–2c** due to the difference in the relative arrangement between the central Cβ-Hβ bond (highlighted in blue) of the allyl ligand and the phenyl ring (red) of the biaryl system (Chart 1). In **2d**, the exo- form is not favored because of the steric repulsion between the phenyl ring of the indenyl group and the phenyl ring of the biaryl.

Chart 1. Endo and exo isomers of Pd(II)–NHC Complexes **2a–2d**

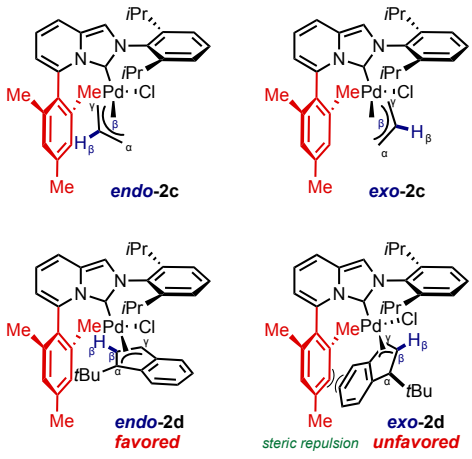

With the library of well-defined Pd(II)–NHC complexes of sterically-restricted imidazo[1,5-*a*]pyridin-3-ylidenes in hand, we next evaluated their reactivity in the Suzuki cross-coupling of nitroarenes (**Table 2**). We were delighted to find that in addition to the highly desirable 1:1 ratio of ligand to Pd, all of the well-defined complexes showed much higher reactivity

than the *in situ* formed Pd–NHCs in the cross-coupling. As such, the yields using complexes **2a**, **2c**, **2d** were 68%, 81% 57%, respectively, after 10 hours (Table 2, entries 1-3), however, the *in situ* protocol gave only 33% yield using the same ligand ImPyMesDipp after 36 hours (Table 1, entry 6).

Table 2. Optimization Using Well-Defined Complexes[a]

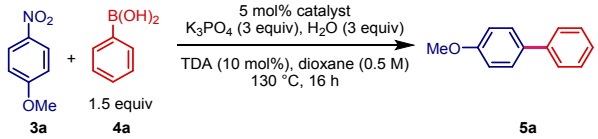

entry	catalyst	yield (%)[b]
1[c]	[(ImPyMesDipp)Pd(allyl)Cl]	68
2[c]	[(ImPyMesDipp)Pd(cin)Cl]	81
3[c]	[(ImPyMesDipp)Pd(1-*t*Bu-ind)Cl]	57
4[c]	[(ImPyTrippMes)Pd(cin)Cl]	74
5	[(ImPyMesDipp)Pd(cin)Cl]	82
6[d]	[(ImPyMesDipp)Pd(cin)Cl]	67
7[e]	[(ImPyMesDipp)Pd(cin)Cl]	47
8[f]	[(ImPyMesDipp)Pd(cin)Cl]	65
9[g]	[(ImPyMesDipp)Pd(cin)Cl]	31
10[h]	[(ImPyMesDipp)Pd(cin)Cl]	35

[a]Conditions: 4-nitroanisole (1.0 equiv), benzeneboronic acid (1.5 equiv), catalyst (5 mol%), K_3PO_4 (3.0 equiv), H_2O (3.0 equiv), TDA (10 mol%), dioxane (0.2 M), 130 °C, 16 h. [b]GC/NMR yield. [c]10 h. [d]w/o water. [e]9 equiv of water. [f]20 mol% TDA. [g]toluene. [h]Cs_2CO_3.

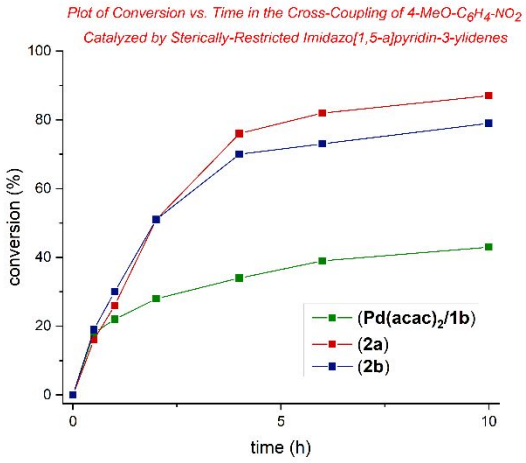

Figure 3. Kinetic profile of the Suzuki-Miyaura cross-coupling of 4-MeO-C_6H_4-NO_2 with phenylboronic acid catalyzed by $Pd(acac)_2$/**1b**, **2a** and **2b** at 130 °C.

Interestingly, ImPyMesDipp supported precatalyst (**2a**) outperformed the ImPyTrippMes ligated precatalyst (**2b**) using the well-defined Pd(II)–NHC complex (81% yield *vs.* 74% yield, Table 2, entry 2 *vs.* 4), affirming that a perfect match of sterics at C5 and N2 positions is needed in the catalytic pocket for optimal results. Extending the reaction time did not improve the yield considerably (Table 2, entry 1 vs. entry 5). Further changes of the reaction conditions gave inferior results (Table 2, entries 6-10). We think that TDA serves as a phase-transfer catalyst. Our results showed both 18-crown-6 and TDA can improve the yields (not shown). Similar to 18-crown-6, TDA binds to potassium cations which leads to a higher concentration of phosphate ion (PO_4^{3-}) in solution.[52]

Kinetic Studies. We next carried out kinetic studies to further compare the catalytic reactivity of the in situ protocol and well-defined Pd(II)–NHC complexes (**Figure 3**). As shown, well-defined complexes showed much superior kinetics as

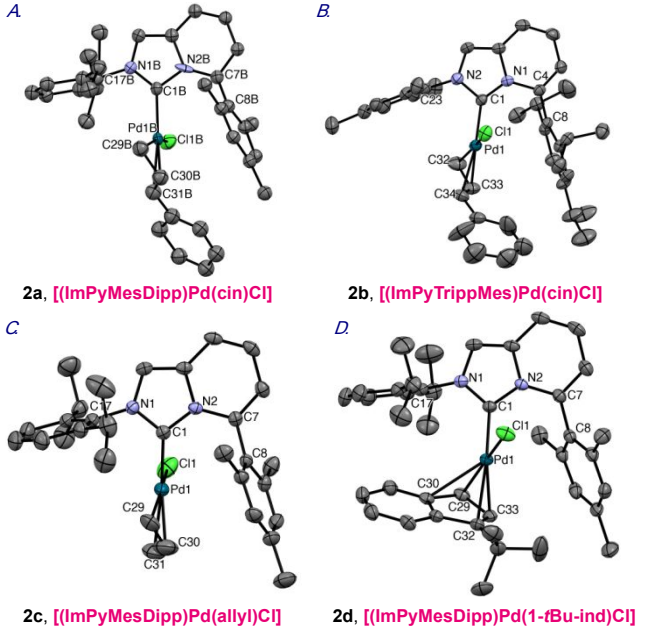

Figure 4. X-ray structure of complex **2a** (A), **2b** (B), **2c** (C), **2d** (D). Hydrogen atoms have been omitted for clarity. See SI for selected bond lengths and angles. CCDC 2174493 (**2a**); CCDC 2174494 (**2b**); CCDC 2174495 (**2c**); CCDC 2174496 (**2d**).

Table 3. Comparison of $C_{carbene}$–Pd Bond Lengths

Pd(II)–NHC	$C_{carbene}$-Pd length (Å)
(IPr)Pd(cin)Cl	2.040(1)
(ImPyMesDipp)Pd(cin)Cl	2.050(2)
(ImPyTripMes)Pd(cin)Cl	2.022(4)
(IPr)Pd(allyl)Cl	2.040(1)
(ImPyMesDipp)Pd(allyl)Cl	2.046(3)
(IPr)Pd(1-*t*Bu-ind)Cl	2.014(3)
(ImPyMesDipp)Pd(1-*t*Bu-ind)Cl	2.030(3)

compared to the *in situ* protocol, consistent with the fast-activation to catalytically-active monoligated Pd(0)–NHCs by the use of cinnamyl ancillary ligand.[58] As such, precatalysts (**2a**) and (**2b**) gave 51% conversion after 2 hours while the $Pd(acac)_2$/**1b** combination only had a conversion of 28%. After 10 hours, 87% of the starting nitroarene was consumed using precatalyst (**2a**), while the reactions using $Pd(acac)_2$ and the same imidazo[1,5-a]pyridinium salt ImPyMesDipp, resulted in less than half conversion after the same reaction of time. Thus, the kinetic studies confirm that well-defined Pd(II)–NHC complexes of imidazo[1,5-*a*]pyridin-3-ylidenes demonstrate much higher reactivity than the *in situ* formed catalysts. Furthermore, the data also establishes that complex [(ImPyMesDipp)Pd(cin)Cl] (**2a**) is more reactive than [(ImPyTrippMes)Pd(cin)Cl] (**2b**). As a further important consideration, ligand ImPyMesDipp is derived from the abundant mesitylene, which is a common feedstock and more readily

available than ImPyTrippMes, which is derived from triisopropylbenzene (*vide infra*).

Table 4. Scope of Suzuki-Miyaura Cross-Coupling of Nitroarenes using Well-Defined [(ImPyMesDipp)Pd(cin)Cl][a]

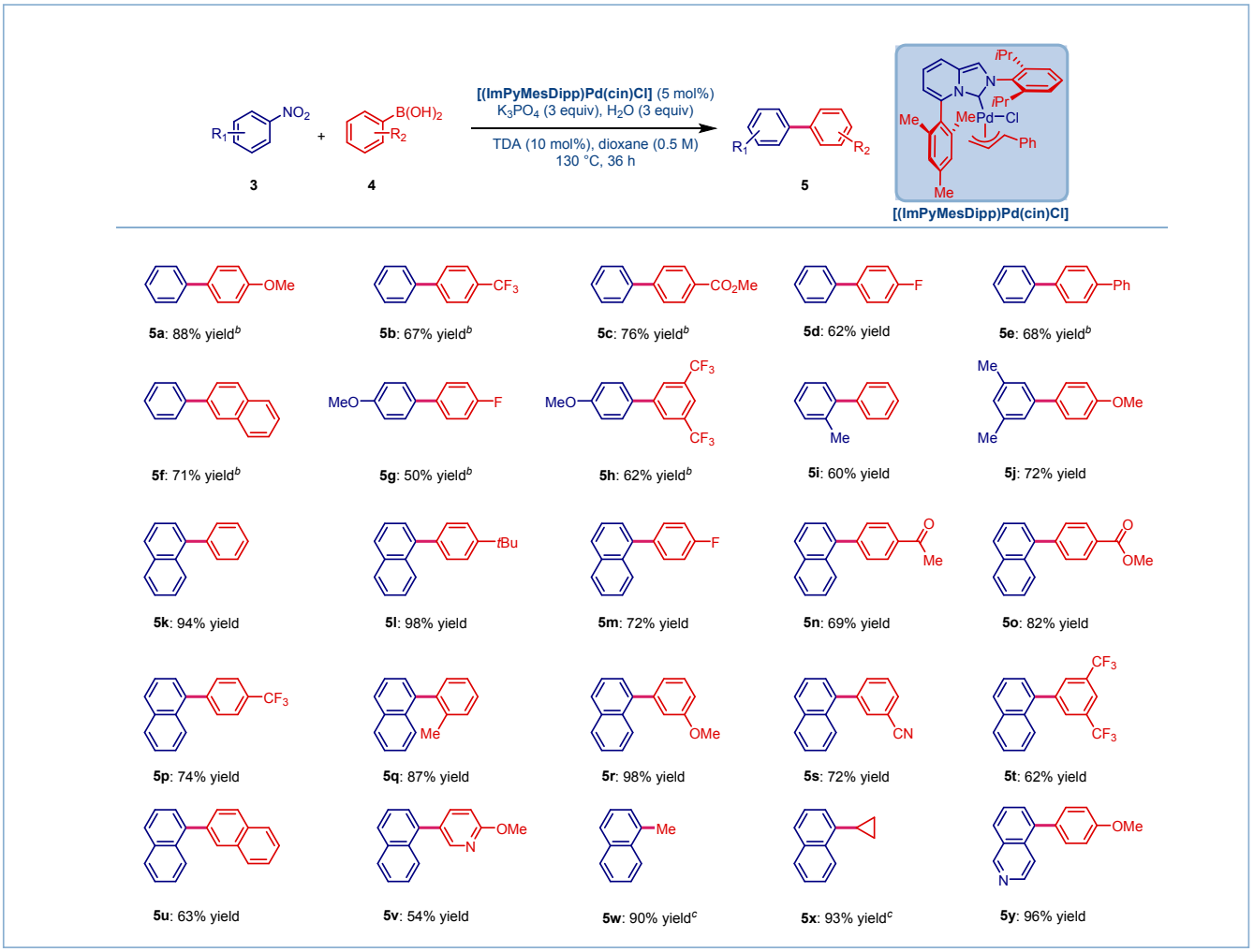

[a]Conditions: nitroarene (1.0 equiv), boronic acid (1.5 equiv), [(ImPyMesDipp)Pd(cin)Cl] (5 mol%), K_3PO_4 (3.0 equiv), H_2O (3.0 equiv), TDA (10 mol%), dioxane (0.2 M), 130 °C, 36 h. [b]16 h. [c]2 equiv of boronic acid. See SI for details.

Characterization of Pd(II)–NHC Complexes. All of the four novel Pd(II)–NHC complexes were fully characterized by x-ray crystallography (**Figure 4**). The C(carbene)–palladium bond lengths are compared with known Pd(II)–NHC complexes ligated with imidazolylidenes, such as IPr (**Table 3**). As shown, the ImPyMesDipp complexes have similar bond lengths to the corresponding [Pd–IPr] complexes.[57-59] However, [(ImPyTrippMes)Pd(cin)Cl] features a shorter C(carbene)–palladium bond length than both [(IPr)Pd(cin)Cl] and [(ImPyMesDipp)Pd(cin)Cl], suggesting a stronger palladium–carbene bond.[59] Furthermore, the Pd–C(allyl) bond lengths are 2.190 Å (Pd–C3) (**2a**), 2.221 Å (Pd–C3) (**2b**), 2.162 Å (Pd–C3) (**2c**), consistent with the previous studies on [(NHC)Pd(R-allyl)Cl] complexes establishing that the longer Pd–C(allyl)–C(3) bond, the easier the activation to monoligated Pd(0).[58]

Topographical steric maps of Pd(II)–NHC complexes **2a**–**2d** determined by the method of Cavallo and co-workers show that [(ImPyMesDipp)Pd(cin)Cl] and (ImPyTripMes)Pd(cin)Cl have $\%V_{bur}$ of 42.1% (Figure 5),[60] which is much higher than that of [(IPr)Pd(cin)Cl] ($\%V_{bur}$ of 34.3%). The % buried volume of [(ImPyMesDipp)Pd(allyl)Cl] and [(ImPyMesDipp)Pd(1-*t*Buind)Cl] is also much higher ($\%V_{bur}$ of 41.7% and 40.9%, respectively).

Crucially, the x-ray analysis in combination with the steric topographical maps reveal that the C5-aryl groups in ImPy are positioned closer to the palladium center than the N2-aryl wingtips (*cf.* IPr). Due to dissymmetry of the ligands, the two quadrants (NE and SE) corresponding to the C5-aryl groups are highly congested, while the other two quadrants (NW and SW) are less sterically-hindered. A closer inspection reveals that the N2-aryl groups have a similar steric effect on the two quadrants (**2a**: 32.9% vs. 37.4%), while the C5-aryl groups give an unsymmetrical steric pressure on the NE and SE quadrants (**2a**: 61.4% vs. 36.8%). These features make well-defined Pd(II)–NHC cinnamyl complexes of imidazo[1,5-*a*]pyridin-3-ylidenes very different

from imidazol-2-ylidenes, such as IPr, which have nearly symmetrical steric distribution around the metal center.[58] This unique catalytic pocket facilitates the approach of substrates to the metal center and reductive elimination.[61]

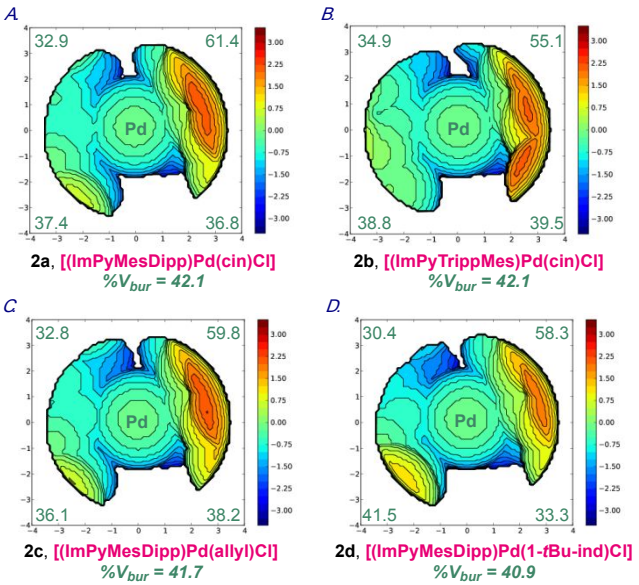

Figure 5. Topographical steric maps of [(ImPyMesDipp)Pd(cin)Cl] (**2a**) (A), [(ImPyTrippMes)Pd(cin)Cl] (**2b**) (B), [(ImPyMesDipp) Pd(allyl)Cl] (**2c**) (C), [(ImPyMesDipp)Pd(1-*t*Bu-ind)Cl] (**2d**) (D) showing % V_{bur} per quadrant.

Catalytic Activity. Next, we examined the scope of the Suzuki cross-coupling of nitroarenes using well-defined Pd(II)–NHC complex (**2a**) (**Table 4**). As shown, a wide range of boronic acids could be coupled with electronically-differentiated nitroarenes by C–NO_2 activation. Thus, boronic acids with electron-donating groups were cross-coupled with electron-neutral (**5a**, **5r**), electron-rich (**5j**) and heterocyclic nitroarenes (**5y**) in high yields under our standard conditions. Furthermore, electron neutral electrophile/nucleophile combinations (**5e**, **5f**, **5k**, **5u**) gave the desired products in good yields. Moreover, electronically-deactivated boronic acids (**5b**, **5c**) smoothly reacted with nitroarenes (**5n**, **5o**, **5p**, **5s**, **5t**), delivering the corresponding biaryls in high yields. Furthermore, electronically-deactivated nitroarenes could be cross-coupled with electronically-deactivated boronic acids (**5g**, **5h**) in good yields. In addition, we note that steric hindrance on either nitroarene (**5i**) or boronic acid component (**5q**) is tolerated. Finally, heterocyclic boronic acids (**5v**) and alkyl boronic acids (**5w**, **5x**) also work well using our protocol.

Ligand Synthesis. In light of the intriguing reactivity of sterically-restricted C5-aryl substituted imidazo[1,5-*a*]pyridin-3-ylidenes, we next developed significantly improved route for ligand synthesis using Ni-catalyzed Kumada cross-coupling and no chromatographic purification (Scheme 2).

Scheme 2. Modular and Chromatography-Free Synthesis of ImPy Ligands via Ni-Catalyzed Kumada Cross-Coupling

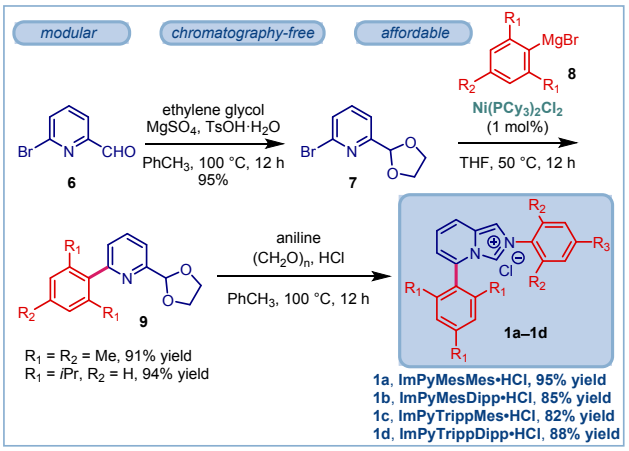

To date, methods to synthesize C5-aryl substituted imidazo[1,5-*a*]pyridinium precursors to ImPy ligands rely on Pd-catalyzed Suzuki cross-coupling to introduce the aryl group at the C5 position.[53,62-63] However, there are three major shortcomings of this frequently used route: (1) mesitylene-2-boronic acid (100g/$206) and 2,4,6-triisopropylbenzeneboronic acid (100g/$401) are expensive;[64] (2) Suzuki cross-coupling of sterically-hindered boronic acids is challenging;[65] (3) chromatographic purification is usually needed due to unsatisfactory yields of the Suzuki cross-coupling.

Having determined the high reactivity of well-defined Pd(II)–NHC cinnamyl complexes of ImPyMesDipp and ImPyTrippMes, we studied new synthetic approach to this class of ligands. As shown in **Scheme 2**, starting from the commercially available aldehyde (**6**), acetal (**7**) could be obtained in near quantitative yield after aqueous work-up. Subsequently, the Ni-catalyzed Kumada cross-coupling between acetal (**7**) and freshly prepared Grignard reagents (**8**) delivered the key intermediates (**9**) in high purities (>95%) and yields (>90%) after extraction, followed by a filtration through a short pad of silica gel. Finally, condensation of (**9**) directly with the corresponding aniline and paraformaldehyde in the presence of HCl furnished the C5-aryl substituted imidazo[1,5-a]pyridinium salts in excellent yields (82-95%). Acetal deprotection of (**9**) in a separate step is not required.

There are several noteworthy features of our synthetic route: (1) significantly more efficient Kumada cross-coupling using cheap and abundant 3d transition metal and at lower catalyst loading (1 mol% Ni vs. 5 mol% Pd); (2) feedstock bromoarenes instead of expensive boronic acids as coupling partners (2,4,6-trimethylbromobenzene, 100g/$32; 2,4,6-triisopropylbromobenzene, 100g/$76), which are significantly cheaper than the corresponding boronic acids;[64] (3) obviating chromatographic purification throughout the synthesis, which permits for a scalable and modular ligand synthesis. We anticipate that this streamlined and economic

route will become a major method in expanding the utility of imidazo[1,5-*a*]pyridin-3-ylidenes in organic synthesis and catalysis.[54]

Orbital Analysis. To provide detailed electronic characterization of sterically-restricted imidazo[1,5-*a*]pyridin-3-ylidene ligands, HOMO and LUMO energy levels of **1a–1d** in comparison with the classical imidazol-2-ylidenes IMes and IPr were determined (**Table 5** and **Figure 6**). It is now well-established that computation of frontier molecular orbitals gives the most accurate determination of ligand nucleophilicity (more

Table 5. HOMO and LUMO Energy Levels (eV) of Imidazo[1,5-*a*]pyridin-3-ylidenes Calculated at the B3LYP 6-311++g(d,p) Level[a]

entry	NHC	HOMO [eV]	LUMO [eV]
1	**1a**	-5.86[b]	-1.24
2	**1b**	-5.91[b]	-1.29
3	**1c**	-5.87[b]	-1.25
4	**1d**	-5.91[b]	-1.30
5	**IMes**	-5.90	-0.33[c]
6	**IPr**	-6.01	-0.48[c]

[a]See SI for details. [b]HOMO-1, in-plane σ-orbital. HOMO: π-donor orbital, **1a**: -5.43 eV, **1b**: -5.49 eV, **1c**: -5.44 eV; **1d**: -5.50 eV. [c]LUMO+2, LUMO+1 due to required symmetry.

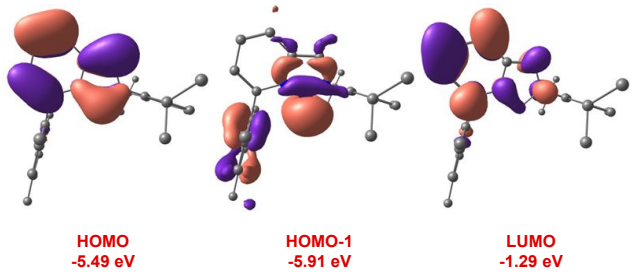

Figure 6. HOMO (π-donating orbital), HOMO-1 (σ-donating orbital) and LUMO (π-accepting orbital) of imidazo[1,5-*a*]pyridin-3-ylidene **1b**. B3LYP 6-311++g(d,p) level. See SI for details.

σ-donating, higher HOMO) and electrophilicity (more π-accepting, lower LUMO), while in some cases π-donation should also be considered. The HOMO-1 (σ-bonding orbital) in the series of ImPyMesMes, ImPyMesDipp, ImPyTrippMes, ImPyTrippDipp are -5.86 eV, -5.91 eV, -5.87 eV, -5.91 eV, which is in the same range as for the standard imidazol-2-ylidene ligands IMes (-5.90 eV) and IPr (-6.01 eV).

Furthermore, the LUMO (π-accepting orbital) in the series of ImPyMesMes, ImPyMeDipp, ImPyTrippMes, ImPyTrippDipp are -1.24 eV, -1.29 eV, -1.25 eV, -1.30 eV, which is much lower than for the standard imidazolylidene ligands IMes (-0.33 eV), IPr (-0.48 eV). The LUMO+1 orbital is located on the N-Ar ring (-0.43 eV, -0.50 eV, -0.45 eV, -0.53 eV) in the series. The results can be compared with the orbital analysis of ImPy carbenes as π-accepting ligands by Shibahara.[66] Interestingly, the HOMO (π-donating orbital) in the series of ImPyMesMes, ImPyMesDipp, ImPyTrippMes, ImPyTrippDipp are -5.43 eV, -5.49 eV, -5.44 eV, -5.50 eV, which is much higher than the π-donating orbital for the standard imidazol-2-ylidene ligands IMes (-6.44 eV), IPr (-6.55 eV).

The data indicate that (1) sterically-restricted imidazo[1,5-*a*]pyridin-3-ylidenes are strongly nucleophilic ligands, as expected for sterically-bulky N-Ar NHC ligands, with σ-donation matching those of IPr and IMes and stronger than phosphines, and (2) significantly better π-acceptors than the standard imidazolylidene IPr and IMes ligands. Furthermore, (3) imidazo[1,5-*a*]pyridin-3-ylidene ligands are characterized by strong π-donating abilities.

Geometry Analysis. To further determine steric properties of this family of ligands and eliminate effects from the crystal packing, analysis of $\%V_{bur}$ of linear [Cu(NHC)Cl] complexes by DFT computations was performed (Figure 7). Cu(I)–NHC complexes were selected as model linear M–NHC complexes.[60]

The %buried volume ($\%V_{bur}$) of [Cu(NHC)Cl] in the series of ImPyMesMes, ImPyMesDipp, ImPyTrippMes, ImPyTrippDipp are 46.8%, 50.1%, 49.8%, 52.4%. Imidazo[1,5-*a*]pyridin-3-ylidenes with C5/N2 steric matching combination are sterically similar ($\%V_{bur}$ = 49.8%-50.1%). C5/N2 substitution with sterically-more demanding substituents results in a decrease in size of catalytic pocket ($\%V_{bur}$ = 52.4%), while C5/N2 substitution with less sterically-demanding substituents leads to low %buried volume in this series of ligands ($\%V_{bur}$ = 46.8%). Quadrant distribution of ImPyMesDipp is 55.3%, 55.3%, 45.0%, 45.0%, and for ImPyTrippMes is 60.9%, 61.4%, 38.5%, 38.2%. The %buried volume values can be compared with the reference imidazolylidene [Cu(IMes)Cl], [Cu(IPr)Cl] with ($\%V_{bur}$) of 36.4%,

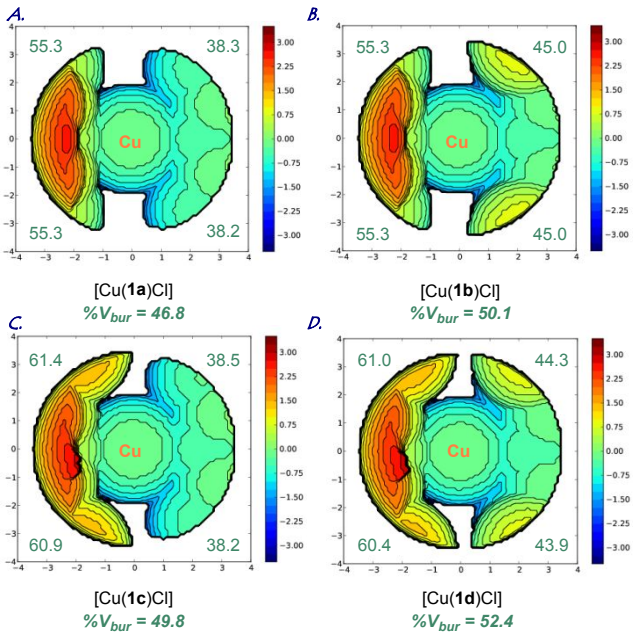

Figure 7. (A-D) Topographical steric maps of linear imidazo[1,5-*a*]pyridin-3-ylidenes [Cu(NHC)Cl] (**1a–1d**) showing % V_{bur} per quadrant. B3LYP 6-311++g(d,p) level. See SI for details.

42.6%. Furthermore, quadrant distribution can be compared with the reference imidazolylidene [Cu(IPr)Cl] of 41.0%, 44.2%, 41.0%, 44.2% and [Cu(IMes)Cl] of 36.4%, 36.4%, 36.4%, 36.4%.

The data indicate (1) significant increase of steric demand of sterically-restricted imidazo[1,5-*a*]pyridin-3-ylidene ligands (ImPyIMesIMes of 46.8% vs. IMes of 36.4%); (2) sterically-fixed conformationally-rigid imidazo[1,5-*a*]pyridin-3-ylidene framework and size-controlled N2-substitution (flexible quadrants). This results in steric features in combination with steric matching between the C5/N2 substituents that are not available in standard imidazolylidenes.

Conclusion

In conclusion, we have reported [(NHC)Pd(cinnamyl)Cl] complexes of ImPy (ImPy = imidazo[1,5-*a*]pyridin-3-ylidene) as sterically-restricted class of precatalysts for cross-coupling reactions. These precatalysts are fast-activating to monoligated Pd(0), feature 1:1 Pd to ligand ratio, are air- and moisture-stable, and do not require glovebox techniques for the synthesis and application. Steric matching of the fixed C5-aryl and flexible N2-wingtip substituents led to the discovery of ImPyMesDipp as highly effective and practical imidazo[1,5-*a*]pyridin-3-ylidene ligand for Pd-catalyzed cross-coupling of nitroarenes by challenging C–NO_2 activation. Crystallographic studies demonstrated the unsymmetrical steric encumbrance of the catalytic pocket crucial for catalytic activity. Computational studies established electronic characteristics of this class of ligands. Importantly, we also disclosed a novel synthetic route to the C5-aryl substituted imidazo[1,5-*a*]pyridin-3-ylidene ligands. Features of our route include efficient and modular Ni-catalyzed Kumada cross-coupling, the use of feedstock starting materials, and chromatography free synthesis, enabling scalable and modular synthesis of conformationally-restricted ImPy ligands. On the basis of high activity of well-defined Pd(II)–NHC cinnamyl complexes of imidazo[1,5-*a*]pyridin-3-ylidenes, we anticipate that these catalysts will find broad utility in activation of unreactive bonds in organic synthesis and catalysis. Studies to expand the scope of reactions enabled by ImPy ligands are ongoing and will be reported in due course.[54]

Conflicts of interest

The authors declare the following competing financial interest: Rutgers University has filed patents on ligands and precatalysts described in this manuscript (US 63/318,481, Mar 10, **2022**).

Acknowledgements

We gratefully acknowledge Rutgers University (M.S.), the NIH (R35GM133326, M.S.), the NSF (CAREER CHE-1650766, M.S.) for generous financial support. The Bruker 500 MHz spectrometer used in this study was supported by the NSF-MRI grant (CHE-1229030). Supplement funding for this project was provided by the Rutgers University – Newark Chancellor's Research Office. We thank the Wroclaw Center for Networking and Supercomputing (grant number WCSS159).

Notes and references

1 A. J. Arduengo, R. Harlow and M. Kline, *J. Am. Chem. Soc.*, 1991, **113**, 361– 363.
2 S. P. Nolan, N-*Heterocyclic Carbenes in Synthesis*, 1st ed., Wiley, 2006.
3 S. P. Nolan, *N-Heterocyclic Carbenes: Effective Tools for Organometallic Synthesis*, 1st ed., Wiley, 2014.
4 S. P. Nolan and C. Cazin, *N-Heterocyclic Carbenes in Catalytic Organic Synthesis*, 1st ed., Thieme, 2017.
5 S. Díez-González, *N-Heterocyclic Carbenes: From Laboratory to Curiosities to Efficient Synthetic Tools*, 2nd ed., Royal Society of Chemistry, 2016.
6 M. N. Hopkinson, C. Richter, M. Schedler and F. Glorius, *Nature*, 2014, **510**, 485–496.
7 D. Munz, *Organometallics*, 2018, **37**, 275-289.
8 F. J. Wang, L. J. Liu, W. F. Wang, S. K. Li and M. Shi, *Coord. Chem. Rev.*, 2012, **256**, 804–853.
9 S. Diez-Gonzalez, N. Marion and S. P. Nolan, *Chem. Rev.*, 2009, **109**, 3612–3676.
10 A. Doddi, M. Peters and M. Tamm, *Chem. Rev.*, 2019, **119**, 6994−7112.
11 Q. Zhao, G. Meng, S. P. Nolan and M. Szostak, *Chem. Rev.*, 2020, **120**, 1981–2048.
12 V. Nesterov, D. Reiter, P. Bag, P. Frisch, R. Holzner, A. Porzelt and S. Inoue, *Chem. Rev.*, 2018, **118**, 9678–9842.
13 M. Soleilhavoup and G. Bertrand, *Acc. Chem. Res.*, 2015, **48**, 256–266.
14 S. Würtz and F. Glorius, *Acc. Chem. Res.*, 2008, **41**, 1523–1533.
15 O. Schuster, L. Yang, H. G. Raubenheimer and M. Albrecht, *Chem. Rev.*, 2009, **109**, 3445–3478.
16 R. H. Crabtree, *Coord. Chem. Rev.*, 2013, **257**, 755–766.
17 Á. Vivancos, C. Segarra, M. Albrecht, *Chem. Rev.*, 2018, **118**, 9493–9586.
18 S. C. Sau, P. K. Hota, S. K. Mandal, M. Soleilhavoup and G. Bertrand, *Chem. Soc. Rev.*, 2020, **49**, 1233–1252.
19 S. De, A. Udvardy, C. E. Czégéni and F. Joó, *Coord. Chem. Rev.*, 2019, **400**, 213038.
20 W. C. Chen, W. C. Shih, T. Jurca, L. Zhao, D. M. Andrada, C. J. Peng, C. C. Chang, S. K. Liu, Y. P. Wang, Y. S. Wen, G. P. A. Yap, C. P. Hsu, G. Frenking, T. G. Ong, *J. Am. Chem. Soc.*, 2017, **139**, 12830-12836.
21 M. Alcarazo, S. J. Roseblade, A. R. Cowley, R. Fernández, J. M. Brown and J. M. Lassaletta, *J. Am. Chem. Soc.*, 2005, **127**, 3290–3291.
22 C. Burstein, C. W. Lehmann and F. Glorius, *Tetrahedron*, 2005, 61, 6207–6217.
23 S. Shi, S. P. Nolan and M. Szostak, *Acc. Chem. Res.*, 2018, **51**, 2589−2599.
24 P. Lei, G. Meng and M. Szostak, *ACS Catal.*, 2017, **7**, 1960−1965.
25 P. Lei, G. Meng, S. Shi, Y. Ling, J. An, R. Szostak and M. Szostak, *Chem. Sci.*, 2017, **8**, 6525−6530.
26 H. Li, C. C. C. Johansson-Seechurn and T. J. Colacot, *ACS Catal.*, 2012, **2**, 1147−1164.
27 T. Zhou, S. Ma, F. Nahra, A. M. C. Obled, A. Poater, L.

Cavallo, C. S. J. Cazin, S. P. Nolan and M. Szostak, *iScience*, 2020, **23**, 101377.
28 T. Zhou, G. Li, S. P. Nolan and M. Szostak, *Org. Lett.*, 2019, **21**, 3304–3309.
29 G. Meng, P. Lei and M. Szostak, *Org. Lett.*, 2017, **19**, 2158−2161.
30 S. Shi and M. Szostak, *Chem. Commun.*, 2017, **53**, 10584−10587.
31 S. Yang, T. Zhou, A. Poater, L. Cavallo, S. P. Nolan and M. Szostak, *Catl. Sci. Technol.*, 2021, **11**, 3189–3197.
32 N. Marion and S. P. Nolan, *Acc. Chem. Res.*, 2008, **41**, 1440−1449.
33 R. D. J. Froese, C. Lombardi, M. Pompeo, R. P. Rucker and M. G. Organ, *Acc. Chem. Res.*, 2017, **50**, 2244−2253.
34 G. R. Peh, E. A. B. Kantchev, J. C. Er and J. Y. Ying, *Chem. - Eur. J.*, 2010, **14**, 4010−4017.
35 V. Lavallo, Y. Canac, C. Prasang, B. Donnadieu and G. Bertrand, *Angew. Chem., Int. Ed.*, 2005, **44**, 5705−5709.
36 N. C. Bruno and S. L. Buchwald, *Buchwald Ligands and Precatalysts: New Palladium Precatalysts For Cross-Coupling Reactions*, Strem Chemicals Inc., 2018.
37 G. A. Olah, R. Malhotra and S. C. Narang, *Nitration: Methods and Mechanism. In Across Conventional Lines*; G. A. Olah and G. K. S. Prakash, Eds.; Wiley, 2003, pp 975–979.
38 M. Kashihara, Y. Nakao, *Acc. Chem. Res.,* 2021, **54**, 2928−2935.
39 K. Muto, T. Okita and J. Yamaguchi, *ACS Catal.*, 2020, **10**, 9856–9871.
40 M. R. Yadav, M. Nagaoka, M. Kashihara, R.-L. Zhong, T. Miyazaki, S. Sakaki and Y. Nakao, *J. Am. Chem. Soc.*, 2017, **139**, 9423–9426.
41 F. Inoue, M. Kashihara, M. R. Yadav and Y. Nakao, *Angew. Chem., Int. Ed.*, 2017, **56**, 13307–13309.
42 M. Kashihara, M. R. Yadav and Y. Nakao, *Org. Lett.*, 2018, **20**, 1655–1658.
43 T. Begum, M. Mondal, M. P. Borpuzari, R. Kar, P. K. Gogoi and U. Bora, *Eur. J. Org. Chem.,* 2017, 3244–3248.
44 K. K. Asahara, T. Okita, A. N. Saito, K. Muto, Y. Nakao and J. Yamaguchi, *Org. Lett.*, 2019, **21**, 4721–4724.
45 Z. Li, Y. Peng, T. Wu, *Org. Lett.*, 2021, **23**, 881–885.
46 B. Feng, Y. Yang and J. You, *Chem. Commun.*, 2020, **56**, 790–793.
47 T. Okita, K. K. Asahara, K. Muto and J. Yamaguchi, *Org. Lett.*, 2020, **22**, 3205–3208.
48 B. Feng, Y. Yang and J. You, *Chem. Sci.*, 2020, **11**, 6031–6035.
49 F. Zhou, F. Zhou, R. Su, Y. Yang and J. You, *Chem. Sci.*, 2020, **11**, 7424–7428.
50 N. Matsushita, M. Kashihara, M. Formica and Y. Nakao, *Organometallics*, 2021, **40**, 2209–2214.
51 W. Chen, K. Chen, W. Chen, M. Liu and H. Wu, *ACS Catal.*, 2019, **9**, 8110–8115.
52 (*a*) K. Chen, W. Chen, X. Yi, W. Chen, M. Liu and H. Wu, *Chem. Commun.*, 2019, **55**, 9287–9290; For the use of TDA as phase-transfer catalyst, see: (*b*) B. P. Fors and S. L. Buchwald, *J. Am. Chem. Soc.*, 2009, **131**, 12898–12899.
53 M. Kashihara, R.-L. Zhong, K. Semba, S. Sakaki and Y. Nakao, *Chem. Commun.*, 2019, **55**, 9291–9294.
54 M. Szostak, T. Zhou and S. Yang, Substituted Imidazol[1,5-a]pyridine N-Heterocyclic Carbene (NHC) Ligands, Catalyst Complexes Thereof, and Methods Using Same. U.S. 63/318,481, Mar 10, **2022**.
55 R.-L. Zhong, M. Nagaoka, Y. Nakao and S. Sakaki, *Organometallics*, 2018, **37**, 3480–3487.
56 C. M. Zinser, F. Nahra, M. Brill, R. E. Meadows, D. B. Cordes, A. M. Z. Slawin, S. P. Nolan and C. S. J. Cazin, *Chem. Commun.*, 2017, **53**, 7990–7993.
57 P. R. Melvin, A. Nova, D. Balcells, W. Dai, N. Hazari, D. P. Hruszkewycz, H. P. Shah and M. T. Tudge, *ACS Catal.*, 2015, **5**, 3680–3688.
58 N. Marion, O. Navarro, J. Mei, E. D. Stevens, N. M. Scott and S. P. Nolan, *J. Am. Chem. Soc.*, 2006, **128**, 4101−4111.
59 M. S. Viciu, O. Navarro, R. F. Germaneau, R. A. Kelly, W. Sommer, N. Marion, E. D. Stevens, L. Cavallo and S. P. Nolan, *Organometallics*, 2004, **23**, 1629–1635.
60 L. Falivene, Z. Cao, A. Petta, L. Serra, A. Poater, R. Oliva, V. Scarano, L. Cavallo, *Nat. Chem.*, 2019, **11**, 872–879.
61 P. Ruiz-Castillo and S. L. Buchwald, *Chem. Rev.,* 2016, **116**, 12564-12649.
62 Y. Kim, Y. Kim, M. Y. Hur and E. Lee, *J. Organomet. Chem.*, 2016, 820, 1–7.
63 D.-A. Park, J. Y. Ryu, J. Lee and S. Hong, *RSC Adv.*, 2017, **7**, 52496–52502.
64 AmBeed, ambeed.com checked on June 26, 2022. For comparison, US prices from Millipore Sigma, sigmaaldrich.com: Mes-B(OH)$_2$/Tripp-B(OH)$_2$: 5g/$90; 5g/$179; Mes-Br/Tripp-Br: 25g/$30; 25g/$102 (checked on June 26, 2022).
65 A. Bruneau, M. Roche, M. Alami and S. Messaoudi, *ACS Catal.*, 2015, **5**, 1386-1396.
66 F. Shibahara, Y. Shibata and T. Murai, *Chem. Lett.*, 2021, **50**, 1892–1900.

